ingegneria sismica
International Journal of Earthquake Engineering
Anno XLIII - Num. 1 - 2026

Real-Time Assessment and Early Warning of Safety Risks in Chemical Processes Based on Bayesian Networks

Shuai Meng[1,*]

[1] Department of Chemical Engineering, Fushun Vocational Technology Institute, Fushun, Liaoning, 113122, China

SUMMARY: *Aiming at the problems of insufficiently comprehensive prediction content and scope as well as the methods of prediction to be improved in the current research on chemical process safety risk prediction, this paper is based on Bayesian network (BN) for real-time assessment and early warning of chemical process safety risk of ammonia synthesis. The constructed risk warning model CNN-ATT-LSTM-BN is divided into two parts: one is the CNN-ATT-LSTM prediction model that combines CNN, LSTM, and attention mechanism, and the other is the safety risk traceability model based on BN. It is shown that the optimal values of linear regression correlation coefficient R2 and root mean square error RMSE of the CNN-ATT-LSTM model are 0.98794 and 0.00088, respectively, which have very high accuracy and are better than the other compared models. Meanwhile, the chemical process risk early warning was realized by risk assessment of the prediction results and risk change curves were obtained. The risk traceability results show that the probability that a safety problem may eventually occur in the chemical production stage is 15.04%, in which the human risk factors (85.74%), followed by mechanical and process factors (22.35%), have the greatest impact on safety. In addition, this paper proposes a scheme to realize risk early warning decision-making by using knowledge mapping, which can be used as a reference for subsequent risk prevention and treatment and other work.*

KEYWORDS: *bayesian network; CNN-ATT-LSTM model; chemical process; safety risk prediction; safety risk tracing*

1 Introduction

China is a major agricultural country, and the market for high-quality chemicals is still expanding together with the large number of chemical manufacturers [1, 2]. Although the chemical industry supplies essential products that support daily life through production and protection, it has also been associated with frequent fires, explosions, poisoning incidents, and other accidents, resulting in heavy casualties, serious property damage to enterprises and the state, as well as substantial harm to natural resources and the ecological environment [3-6]. Literature [7] examined hazardous chemical accidents in China from 2000 to 2006 and found that such events occurred in large numbers, most of them concentrated in the southeastern coastal region, where losses of life and property were particularly severe. The reference [8] noted that China has become one of the largest producers and consumers of hazardous chemicals, and the hazardous chemicals industry is one of the sectors with the highest level of risk. Two major ones are the Qingdao Crude Oil Spill and Explosion on November 2 and the

*18642300740@163.com
https://doi.org/10.65102/is2026384
Published: 30 April, 2026

Tianjin Port Fire and Explosion on August 12.Literature [9] pointed out that accidents in chemical production processes are prone to cause serious casualties, property damage, and environmental pollution, and investigated chemical accidents that occurred in South Korea during the period of January 2008 to June 2018, and systematically described their causes. Literature [10] describes the harm caused by chemical processes to the environment, pointing out that chemical substances and industrial wastes alter the chemical-physical parameters of habitats, interfere with the natural cycle of substances in the biosphere, and negatively affect nature's self-purification process.

The causes of these accidents are manifold. One important reason is that a considerable number of enterprises still operate with a relatively low level of technical equipment, which restricts the automation of control systems and the safety design of devices [11, 12]. In addition, the professional competence of practitioners is not always ensured, their awareness of safety remains insufficient in some cases, and both safety knowledge and safe working habits still require improvement [13, 14]. From a process perspective, many enterprises lack adequate knowledge of reaction risks, apply unsound safety regulations, and rely on outdated safety-management practices, which directly lead to nonstandard safety-disposal measures [15, 16]. Literature [17] analyzed 14 major chemical accidents by using OVOSview software and concluded that weak process-safety culture, deliberate violations of operating procedures, and insufficient safety training were the most common causes. Literature [18] investigated factors that may induce process-safety accidents in the U.S. chemical manufacturing sector and showed through accident-data analysis that the primary causes were related to preventive maintenance, inadequate protective measures, weak control measures, and similar issues. Literature [19] studied chemical-process accident cases in order to identify the causes of chemical-equipment accidents, and the results indicated that the most frequent contributing factors involved pipelines, reactors, tanks, and process vessels, while the table in that study also summarized additional accident-related factors. Literature [20] discussed deficiencies in safety management within chemical enterprises and stressed the importance of risk management for chemical processes, covering all aspects of industrial-unit operation and contributing effectively to the prevention of chemical-process accidents. Therefore, real-time assessment and early warning of safety risks in chemical processes are of considerable importance.

The implementation of industrial 4.0 related policies at the national level around the world has seen the rise of artificial intelligence as an inseparable part of the development of industry 4.0 [21, 22]. Literature [23] reviewed the features of AI adoption in the Industry 4.0 environment, and determined the ways of its implementation in practice, and concluded that AI has had a positive contribution to the business transformation. Literature [24] investigated the critical importance of AI in ensuring the effectiveness of Industry 4.0 through the analysis of the literature and revealed that AI has tremendous benefits and is gradually enabling the achievement of various goals of Industry 4.0. The fact that safety takes up a very crucial position in the process of chemical production makes the application of AI methods to minimize risk and enhance safety in the process of chemical manufacturing one of the most trending tendencies [25-27]. Literature [28] pointed out the high potential of AI as a new technology of decreasing energy usage and environmental impact during the chemical production processes and provided the future research outlook. Literature [29] addressed issues of safety in chemical procedures and to address such issues, suggested the safety-production monitoring system based on deep learning and artificial intelligence technology, which had the ability to implement enterprise safety monitoring, early warning, and smart operations. Being one of the crucial artificial-intelligence technologies, Bayesian networks can also be used in real-time safety risk evaluations and initial warnings concerning chemical process [30, 31].

Bayesian network (BN) is a graphical network based on probabilistic reasoning, which consists of nodes and edges [32]. Nodes represent random variables, which can be a variety of factors that may affect safety, such as equipment state, personnel behavior, etc., and edges represent conditional dependencies between variables [33-35]. Through this network structure, the mutual influences among factors can be visualized, and then reasoned and analyzed using probabilistic and graph theoretic methods [36, 37]. In the real-time assessment and early warning of chemical process safety risk, Bayesian network can easily integrate multiple factors affecting safety together for analysis, can clearly show the relationship between these factors, accurately assess the overall safety risk level of the chemical process, and issue an early warning, which provides support for the realization of the chemical process safety [38-41].

Regarding Bayesian-network research on safety-risk assessment and early warning in the chemical industry, literature [42] established a BN model for chemical-plant explosion accidents in order to analyze potential accident causes in the chemical sector. Based on the assessment results, it found that direct factors exerted the strongest influence on accident consequences, whereas unsafe conditions had a greater effect than unsafe behaviors. Literature [43] proposed a framework for the dynamic assessment of chemical accidents and developed an accident-specific BN model that integrates historical data with expert experience to support prevention, management, and real-time warning; the results showed that this approach had a significant impact on emergency response and accident outcomes. Literature[44] attempted to develop an improved text-mining method and constructed a BN model to analyze safety-risk factors, presenting the interrelationships among those factors and verifying that the method can rapidly and efficiently extract key information from accident reports so as to provide managers with insights and recommendations. Literature [45] examined the application of BN in chemical safety assessment and showed that BN can provide comprehensive qualitative, quantitative, and dynamic graphical modeling of accident scenarios, thereby enabling more dynamic, accurate, and practical risk assessment in chemical plants. Literature [46] proposed a dynamic BN-based methodology, which was validated as a solid scientific basis for risk-management decisions in typical chemical production processes within chemical enterprises by applying it to the real-time calculation and assessment of residual risks in chemical production processes. Literature [47] discussed the identification and analysis of chemical-safety risk factors by combining an improved LDA topic model with a Bayesian network, revealing both the correlation and the causality among risk factors. Besides BN, other approaches have also been adopted in the safety early warning of chemical processes. For example [48] constructed a dual-mode cooperative early-warning system by integrating multi-source information from “conventional parameter monitoring-risk situation awareness” with cusp-mutation theory and risk-entropy analysis, thereby providing a strong basis for accident early warning.

In this paper, a risk warning model CNN-ATT-LSTM-BN, which includes CNN-ATT-LSTM prediction model and BN risk tracing model, is proposed for the safety risk warning of chemical process, and the synthesis tower process of ammonia synthesis section of a chemical enterprise is used as an experimental object to verify the validity of the model by predicting parameters such as hydroxide-oxygen ratio, inlet pressure of the synthesis tower, the first bed temperature of the synthesis tower, the second bed temperature of the synthesis tower, the condensate flow rate of feedwater heat exchanger, the process gas flow rate of pipeline, and the corresponding risk levels. , feed water heat exchanger condensate flow rate, pipeline process gas flow rate, and other parameters with corresponding risk levels, as well as tracing the influencing factors on the risk to verify the effectiveness of the model. Finally, a chemical process safety risk early warning decision-making scheme is designed based on knowledge mapping.

2 Method

In order to realize the real-time assessment and early warning of chemical process safety risk, this chapter establishes a combined prediction model CNN-ATT-LSTM-BN, which consists of two parts: the chemical process safety risk prediction model CNN-ATT-LSTM, and the safety risk traceability model based on BN.

2.1 CNN-ATT-LSTM Prediction Modeling

2.1.1 Convolutional Neural Networks

Convolutional neural networks (CNN) is a deep neural network structure based upon convolutional computation. It has an input layer, an optional one or more hidden layers, and an output layer. The input can be one-dimensional or multi-dimensional depending on the task. Most often, the hidden section of a CNN consists of convolutional layers, activation functions, pooling layers, and fully connected layers. Convolutional layers can be divided into one-dimensional, two-dimensional and three-dimensional types, depending on the dimensionality of the input data. Following the extraction of features by convolution on the input, a nonlinear transformation is applied by the activation function. These feature maps are subsequently fed into the pooling layer to select and reduce the information so that the data can be compressed. Popular pooling methods are max pooling and average pooling and they return the maximum value and mean value of the feature map respectively. A pooling layer is typically located between two consecutive convolutional layers; however, the fully connected layer is positioned at the end of the last pooling layer and connects all the features extracted to the classifier to produce the final classification outcome.

Let X_t , $t=1,2,\ldots,n$, denote a time-series set, where $X_t \in R^k$ represents the k -dimensional vector at time t . A filter in the convolution layer performs a sliding convolution on the time series with a window of width h , thereby producing a new feature c_t . The convolution operation can be written as follows:

$$c_t = f\left(WX_{t:t+h-1} + b\right) \tag{1}$$

where $W \in R^{hk}$ is the weight term, $X_{t:t+h-1}$ denotes the time-series segment from time t to time $t+h-1$, b is the bias term, and f is the activation function. When a filter is applied to an n-order time series with a window width h, $n-h+1$ new features are generated to form a feature map c:

$$c = \left[c_1, c_2, \ldots, c_{n-h+1}\right] \tag{2}$$

The feature map is then fed into the max-pooling layer, where the largest feature value is selected as the output. The role of max pooling is to preserve the most informative features while reducing the number of parameters and the computational burden, thereby alleviating overfitting and improving the model's generalization capability. After several rounds of convolution and pooling, the fully connected layer sends the extracted features to the classifier, and the whole procedure is completed.

2.1.2 Long and short-term memory networks

Long Short-Term Memory (LSTM) has been developed as a better version of recurrent neural

network (RNNs). It uses memory units instead of ordinary hidden nodes in an RNN, which solves the problem of gradient-vanishing and gradient-explosion after numerous iterations of RNN training. In comparison to the conventional RNN, the LSTM is more appropriate to learn a temporal pattern with long-term dependencies and is thus more appropriate to be used when classifying and forecasting time series.

An LSTM unit includes an input gate, a forget gate (f), an update gate (u), and an output gate (o). The input data of the input layer consist of the state output value a_{t-1} from the previous moment, the output value c_{t-1} of the previous memory cell, and the time-series value x_t at the current moment. The forget gate combines a_{t-1} and x_t to obtain its output, which can be expressed as

$$F_f = \sigma\left(W_f\left[a_{t-1}, x_t\right] + b_f\right) \tag{3}$$

where σ denotes the activation function, W_f is the weight matrix of the forget gate, and b_f is the bias term. The forget gate enables the network to selectively discard information and avoid saturation. The update gate is then used to determine which part of the information in F_u should be updated, and the tanh layer is adopted to refresh the candidate value $\tilde{c}_t$ of the memory cell.

$$F_u = \sigma\left(W_u\left[a_{t-1}, x_t\right] + b_u\right) \tag{4}$$

$$\tilde{c}_t = \tanh\left(W_c\left[a_{t-1}, x_t\right] + b_c\right) \tag{5}$$

Next, update c_{t-1} to c_t:

$$c_t = F_u \cdot \tilde{c}_t + F_f \cdot c_{t-1} \tag{6}$$

The forgetting gate is used to forget some of the old unit information, the updating gate and the tanh layer are used to add new candidate unit information to the memory cell, and the combination of these three layers generates new unit information c_t. Subsequently, F_O is obtained after inputting a_{t-1} and x_t into the output gate:

$$F_o = \sigma\left(W_o\left[a_{t-1}, x_t\right] + b_o\right) \tag{7}$$

Meanwhile, the cell information c_t is input into the tanh layer to obtain the vector $\tanh\left(c_t\right)$ with values ranging from -1 to 1. Finally, the activation value a_t at the moment of t is obtained by combining F_O and $\tanh\left(c_t\right)$, and the final output value is obtained by inputting a_t into the activation function:

$$a_t = F_o \cdot \tanh\left(c_t\right) \tag{8}$$

$$y_t = g\left(a_t\right) \tag{9}$$

where g is an activation function, common activation functions are the σ activation function, the tanh activation function and the ReLu activation function to name a few.

2.1.3 Attention mechanisms

Attention Mechanism (AM) operates through allocating various weights and is designed to mimic the way the human brain allocates attention. In the application discussed in the present paper, the attention mechanism can be seen as a strategy of allocating resources that guide computation resources to more important tasks. In this manner, it assists in reducing the overload of information when the computational capacity is restricted and thus enhances the performance of the model as well as its precision. Figure 1 depicts the structure of the LSTM model with the attention mechanism.

Where X_t and h_{t-1} are the inputs to the LSTM model, h_t is the output of the LSTM hidden layer, α_t is the probability weight assigned by the attention mechanism to the output value of each hidden layer, $\alpha_t \in R^k$, and α_t^p measures the significance of the p th feature at the moment t. The updated h_t is $\tilde{h}_t = \left(\alpha_t^1 x_t^1, \alpha_t^2 x_t^2, \cdots, \alpha_t^k x_t^k\right)$. Finally $\tilde{h}_t$ is fed into the fully connected layer to get the final output Y.

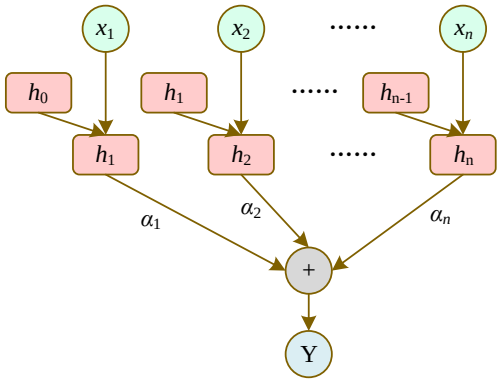

Figure 1: Structure of LSTM model combined with Attention Mechanism

2.1.4 Overall structure of the CNN-ATT-LSTM model

The detailed structure of the CNN-ATT-LSTM prediction model is presented in Fig. 2. The model mainly contains an input layer, two CNN layers, an Attention layer, an LSTM layer, a fully connected layer, and an output layer.

(1) Input layer

The input layer mainly inputs fixed format data into the model. In this model, since the input data enters the CNN1 layer first, in order to match the structure of the CNN1 layer, the structure of the input layer is: $Input_{size} = (Timestep, 1, Dims)$. $Timestep$ represents the timestep of the input data. 1 means that all inputs from the input layer to the CNN1 layer are 1 point in time $Dims$. The $Dims$ represents the dimension of the input data. According to the structure of the input layer, it can be seen that the vector dimension of the input is $(1, Dims)$, and an input needs to be done as many times as $Timestep$ times.

(2) CNN layer

The first CNN layer contains 32 convolution kernels with a kernel size of $1*Dims$, while the second CNN layer contains 21 convolution kernels with a kernel size of 1×321\times

321×32. The convolution operation of the CNN layer is implemented according to Equation (1).

(3) Attention layer

Since a Flatten layer is added to the CNN2 layer to spread the data, plus the CNN2 has 21 convolutional kernels, the structure of the Attention layer input data is: $ATT_{size} = (Timestep, 1, 21)$.

The Attention layer first computationally processes the inputs of the CNN2 layer through a fully connected layer to obtain the weight matrix W and the bias vector b, and the values to be predicted are used as query vectors, which are computed through Eqs. (10) to (11) to obtain the attention distribution a_i:

$$a_i = p(z = i | X, q) = soft\max(s(X_i, q)) = \frac{\exp(s(X_i, q))}{\sum_{j=1}^{N} s(X_i, q)} \tag{10}$$

$$s(X_i, q) = v^T \tanh(WX_i + Uq) \tag{11}$$

where $X = [x_1, \ldots, x_N]$ denotes the N input information and q is the object to be queried in context. The attention distribution a_i represents the probability that this i th input message is selected when an index position $z = i$ is determined to select the i th input message, given X and q. The $s(X_i, q)$ is the attention scoring mechanism.

The assignment of each feature is then realized by equation (12):

$$Attention(q, X) = \sum_{i=1}^{N} a_i X_i \tag{12}$$

The Softmax function in Eq. (10) calculates the similarity between inputs and outputs, and Eq. (12) implements the weight assignment of feature metrics. Through the Attention layer, some features that are relatively important to the prediction results are given more attention.

(4) LSTM layer

For a memory block, there are three gates, which correspond to three Sigmoid functions and one tanh function, each of which can be regarded as a feedforward network layer. The Units of the LTSM layer of this model are set to 32, which means that there are 4 feedforward network layers with 32 neurons.

The computation of the LSTM layer is performed using Eqs. (3) to (9), where the Sigmoid function is computed as follows:

$$Sigmoid = \frac{1}{1 + e^{-x}} \tag{13}$$

The tanh function is calculated as follows:

$$\tanh\left(\frac{e^{x} - e^{-x}}{e^{x} + e^{-x}}\right) \tag{14}$$

Sigmoid function and tanh function represent the strength of each control gate. The temporal features in the data are fully extracted through the LSTM layer.

(5) Fully connected layer and output layer

The structure of the fully connected layer is set to 2 neurons and the dimension of the output layer is 2.

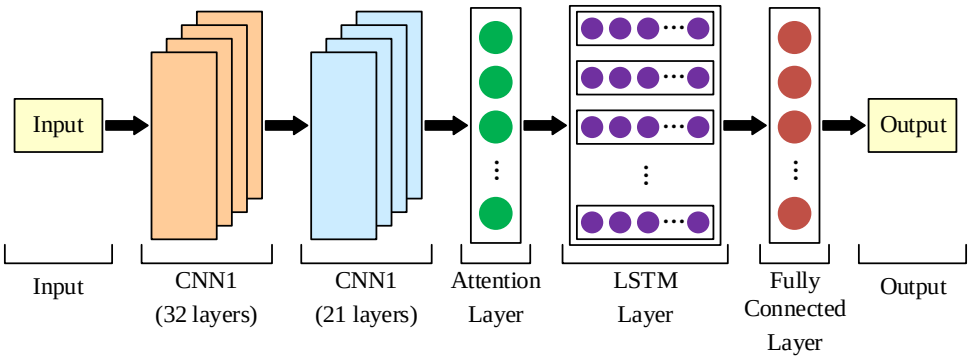

Figure 2: CNN-ATT-LSTM model structure

2.2 Bayesian networks

The Bayesian network (BN) is a mathematical model, which reflects and depicts correlations or causal connections between factors in data using probability theory as a basis. It has probabilistic reasoning as its inferential basis, and graph theory as its representation. A Bayesian network is made up of two sections. The first one is a directed acyclic graph (DAG), which means that a node cannot be an ancestral node to itself. The DAG has several nodes linked by directed line segments, also known as directed edges. These nodes signify the variables in the problem to be analyzed, and the directed edges indicate the dependent or causal relationships between these variables. The second section is the conditional probability table (CPT) and it offers the quantitative representation in the Bayesian network and it is applied to represent the level of confidence between child nodes and parent nodes. Every node is associated with a given probability distribution table.

2.2.1 Bayesian network modeling approach

The specific modeling process for Bayesian networks is roughly as follows:

(1) Determine the influencing factors:

1) Determine the model dependent and independent variables.

2) Obtain observations of the model's influencing factors.

3) Screen the variables.

(2) Determine the structure of the network: usually it can be divided into two kinds: manual construction by consulting experts and construction through data analysis.

(3) Determine the network parameters, i.e., determine the probability distribution table of network nodes.

Bayesian network construction focuses on the determination of its structure and parameters, i.e., structure learning and parameter learning. Common modeling methods are:

(1) Expert construction method, where the network structure is constructed manually by consulting experts in the field or by experts directly determining the nodes, structure, parameters, etc. contained in the Bayesian network.

(2) Data learning method, under the condition of determining the relevant influencing factors of the Bayesian network, i.e., the nodes, the structure and parameters of the Bayesian network are automatically generated through a large amount of data training and learning algorithms.

(3) Hybrid construction method, which utilizes the initial formation of nodes and structures constituting the Bayesian network through the expert construction method, while the parameters are generated through the data learning method and adjusted to the final Bayesian network.

2.2.2 Bayesian network structure learning

The core of structure learning in Bayesian networks is to reveal both qualitative and quantitative relationships between variables. Structure learning can be divided into two steps: model selection and model optimization.

Model selection is usually judged by:

(1) Likelihood function model selection, by preferring the parametric log-likelihood function as the scoring function.

(2) Bayesian model selection, using Bayesian parameter estimation as the criterion for coming Bayesian network model selection.

(3) Large-sample model selection, which is based on the Bayesian information criterion for model selection, also known as the BIC scoring method, is one of the most commonly used scoring functions.

(4) Other model selection, including the shortest description length MDL scoring function, Akaike information criterion AIC scoring function and so on.

Methods of model optimization usually include:

(1) Scoring-based search strategy

The basic idea of the scoring-based structure learning method is to traverse all possible Bayesian network structures and adopt a criterion to measure and compare all of them, so as to find out the best structure among them. The key point of the method is: choosing a suitable search strategy and scoring function. Common scoring functions include: BIC scoring function, K2 scoring function, MDL minimum description length and so on. Common search strategies include: K2 algorithm, hill-climbing algorithm, A* algorithm, particle swarm optimization algorithm, and methods based on genetic evolution, artificial bee colony algorithm and so on.

(2) Constraint-based search strategies

The core idea of constraint-based structural learning methods is to test the dependence or independence between variables based on statistics and information theory, in which the focus is on the conditional independence between variables, and then construct a directed acyclic graph. Common search strategies include SGS algorithm, PC algorithm, TPDA algorithm and so on.

2.2.3 Bayesian network parameter learning

Bayesian network parameter learning refers to determining the probability distributions of individual nodes, including prior distributions and conditional probability distributions, on the basis of a given Bayesian network structure and dataset. Two common methods are used for parameter learning on complete datasets: the maximum likelihood estimation (MLE) method and the Bayesian estimation (BE) method. Both approaches require the data samples to satisfy the condition of independent and identically distributed observations. That is, given a dataset $D=\left(d_1,d_2,\cdots,d_m\right)$,where D contains m samples and $d_i=\left\{d_{i1},d_{i2},\cdots,d_{in}\right\}$, $i=1,2,\cdots,m$, then each sample in D satisfies the following two conditions:

(1) Each sample in D is independent of each other given the parameter θ, i.e.:

$$P(D\mid\theta)=\prod_{i=1}^{m}P\left(d_i\mid\theta\right) \tag{15}$$

(2) Each sample d_i has the same conditional probability distribution $P(d_i \mid \theta)$.

Maximum likelihood estimation (MLE) is a method of parameter estimation based on the degree of likelihood between the sample data and the predicted parameter, with the formula:

$$\theta^* = \arg\max_{\theta} L(\theta \mid D) \tag{16}$$

where $L(\theta \mid D) = P(D \mid \theta)$ is the likelihood function of θ.

Consider a Bayesian network consisting of n variables $X = \{x_1, x_2, \cdots, x_n\}$, and let the variable x_i have r_i values, and the combinations of the values of its parent node $pa(x_i)$ have a total of q_i values, if x_i has no parent node , then $q_i = 1$, and the network parameters $\theta = \{\theta_{ijk} \mid i = 1, \cdots, n; j = 1, \cdots, q_i; k = 1, \cdots, r_i\}$, where $\theta_{ijk} = P(x_i = k \mid pa(x_i) = j)$. Taking the logarithm of $L(\theta \mid D)$ gives:

$$\ell(\theta \mid D) = \log L(\theta \mid D) = \log \prod_{i=1}^{m} P(d_i \mid \theta) = \sum_{i=1}^{n} \sum_{j=1}^{q_i} \sum_{k=1}^{r_i} m_{ijk} \log \theta_{ijk} \tag{17}$$

where m_{ijk} is the number of samples in data D that satisfy $x_i = k$ and $pa(x_i) = j$. For any fixed i and j, since $\sum_{k=1}^{r_i} \theta_{ijk} = 1$, when θ_{ijk} takes the following values:

$$\theta_{ijk}^* = \begin{cases} \dfrac{m_{ijk}}{\sum_{k=1}^{r_i} m_{ijk}}, & \text{If } \sum_{k=1}^{r_i} m_{ijk} > 0 \\ \dfrac{1}{r_i}, & \text{If not} \end{cases} \tag{18}$$

The expression $\sum_{k=1}^{r_i} m_{ijk} \log \theta_{ijk}$ is maximized, and thus $\ell(\theta \mid D)$ is maximized. Therefore, θ_{ijk}^* is the maximum likelihood estimate of θ_{ijk}, which intuitively has:

$$\theta_{ijk}^* = \frac{\begin{array}{c}\text{The number of elements in } D \\ \text{satisfying } x_i = k \text{ and } pa(x_i) = j\end{array}}{\begin{array}{c}\text{The number of elements in } D \\ \text{satisfying } pa(x_i) = j\end{array}} \tag{19}$$

Bayesian estimation treats the parameter to be estimated as a random variable and fully considers the influence of prior knowledge on parameter selection, thus making it more reasonable than MLE. Intuitively, it can be argued that Bayesian estimation satisfies:

$$\theta_{ijk}^* = \frac{m_{ijk} + \alpha_{ijk}}{\sum_{k=1}^{r_i} \left(m_{ijk} + \alpha_{ijk} \right)} \tag{20}$$

$$\theta_{ijk}^{*} = \frac{\begin{array}{l}\text{Number of values in } D \text{ satisfying } x_i = k \text{ and } pa(x_i) \\ = j + \text{Number of values satisfying} \\ \text{corresponding prior knowledge}\end{array}}{\begin{array}{l}\text{Number of values in } D \text{ satisfying } pa(x_i) \\ = j + \text{Number of values satisfying} \\ \text{corresponding prior knowledge}\end{array}} \tag{21}$$

2.2.4 Bayesian network reasoning

Bayesian network inference is essentially a decomposition of the joint distribution based on independent relationships between variables, which can be roughly categorized into three types: inference on the posterior probability problem, inference on the maximum a posteriori hypothesis problem, and inference on the maximum possible explanation problem. Among them, the most frequently concerned is the a posteriori probability problem reasoning.

Reasoning in a posteriori probabilistic problems is a probabilistic problem of predicting the possible values of an unknown variable based on known conditions such as the known values of a variable. In this context, E is often used to represent the known variable, called the evidence variable. The variable for which the posterior probability needs to be computed is represented by Q and is called the query variable. The posterior distribution that needs to be calculated can then be visualized as:

$$P(Q \mid E = e) \tag{22}$$

2.3 BN-based Security Risk Traceability Modeling

This paper proposes a BN-based safety-risk traceability model to solve the issue of real-time evaluation and pre-warning of safety threats in chemical processes, as shown in Figure 3. When computing the model, the frequency of events in the case data is used to determine the probability of the occurrence of an event, the prior probability of every node is estimated, and subsequently, the joint probability of the nodes is computed. Subsequently, all the probabilities of the nodes are entered into the Bayesian network to conduct safety-risk traceability and predictive diagnostic analysis of chemical processes.

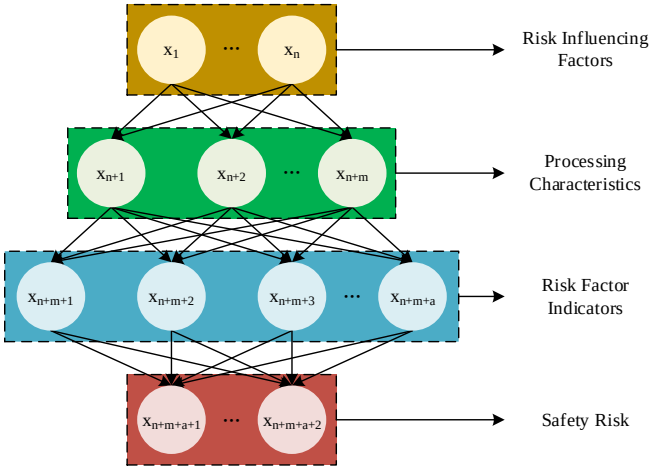

Figure 3: Bayesian network structure

3 Results and Discussion

The process in question to test the effectiveness of the chemical-process safety risk early-warning model incorporating the CNN-ATT-LSTM with a Bayesian network is the synthesis tower process in the ammonia production section of a chemical company operating in Yunnan Province, China, chosen in this chapter as the validation case.

3.1 Analysis of CNN-ATT-LSTM model prediction results

3.1.1 Model evaluation indicators

The root mean square error ($RMSE$) and the coefficient of determination (R^2) are chosen as the assessment criteria to assess predictive performance in linear regression analysis. RMSE quantifies the difference between predicted values and observed values; with the estimation of the same variable, lower $RMSE$ means greater predictive precision. R^2 indicates the level of fitness between the fitted results and the actual data, and a value close to 1 means that the model fits the data well. The specific formulas are presented below:

$$RMSE = \sqrt{\frac{1}{N}\sum_{t=1}^{N}\left(y_{pred}(t) - y_{act}(t)\right)^2} \tag{23}$$

$$R^2 = 1 - \frac{\sum_{t=1}^{N}\left(y_{pred}(t) - \bar{y}\right)^2}{\sum_{t=1}^{N}\left(y_{act}(t) - \bar{y}\right)^2} \tag{24}$$

where N represents the total number of predictions. $y_{pred}(t)$, $y_{act}(t)$ represent the predicted and actual values at the moment of t , respectively. $\bar{y}$ represents the mean value.

3.1.2 Analysis of the results of the prediction of chemical process parameters

In order to examine the impact of the number of training iterations on the performance of the CNN-ATT-LSTM model, ten different iteration settings were used and their comparison outcomes are given in Table 1.

The findings indicate that the model performs with the highest prediction rate when the number of training rounds is equal to 550 and the maximum number of iterations is 5500. The model parameters and the number of iterations were eventually determined after testing.

Table 1: Comparison of the effects of training rounds

Number of training rounds	400	450	500	550	600	650
RMSE	0.00135	0.00168	0.00095	0.00088	0.00090	0.00093
R^2	0.90237	0.89369	0.92816	0.98794	0.98236	0.92753

Six parameters in the chemical process of the synthesis tower were selected as risk warning factors, and the six groups of parameters were predicted based on the CNN-ATT-LSTM prediction model, and the results of the parameter prediction are shown in Fig. 4. Among them, (a)~(f) denote the prediction results of hydrogen-oxygen ratio, inlet pressure of synthesis tower, first bed temperature of synthesis tower, second bed temperature of synthesis tower, condensate

flow rate of feedwater heat exchanger, and process gas flow rate of pipeline, respectively, and the same as the latter. It can be seen that the deviation between the predicted and actual values of the six chemical process parameters is extremely small, and the model predicts better.

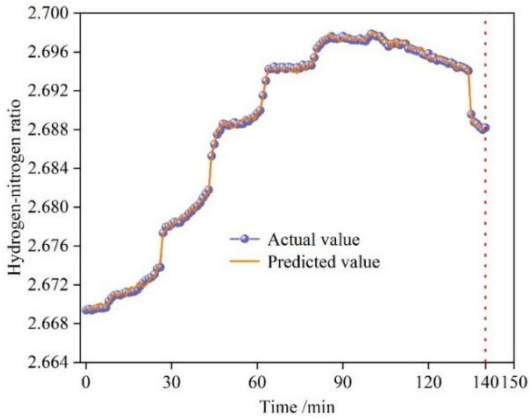

(a) Hydrogen-nitrogen ratio

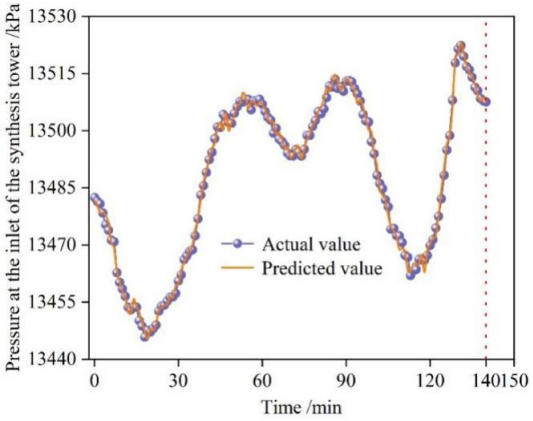

(b) Pressure at the inlet of the synthesis tower

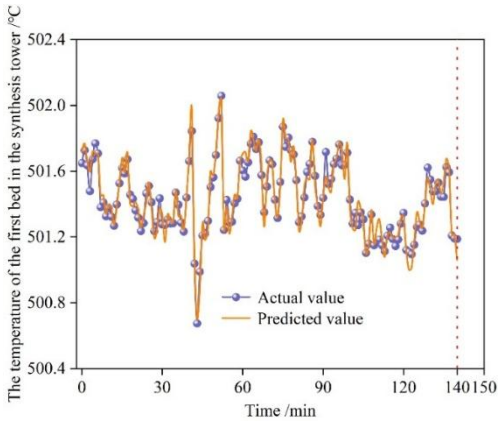

(c) The temperature of the first bed in the synthesis tower

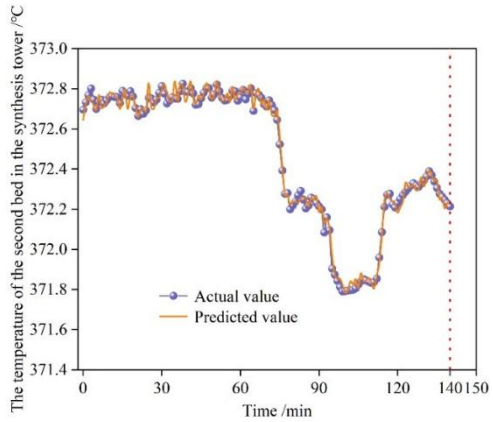

(d) The temperature of the second bed in the synthesis tower

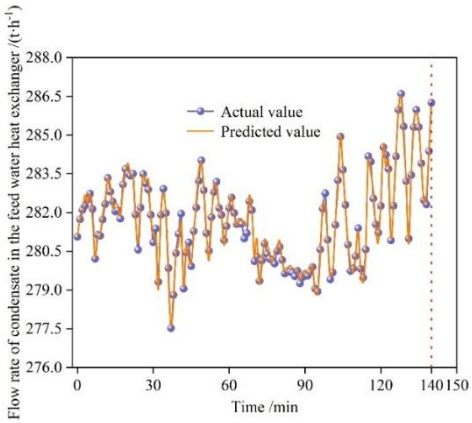

(e) Flow rate of condensate in the feed water heat exchanger

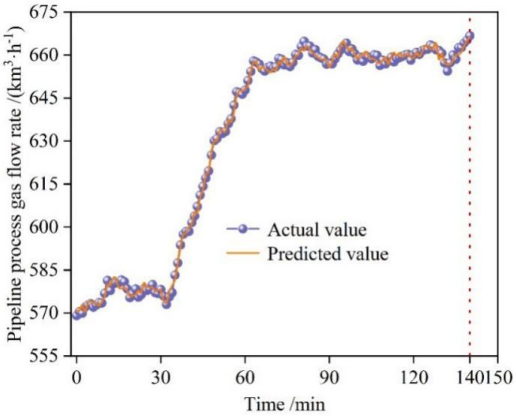

(f) Pipeline process gas flow rate

Figure 4: Prediction results of the CNN-ATT-LSTM model

To further evaluate the effectiveness of the CNN-ATT-LSTM prediction framework, three additional models, namely the CNN model, the LSTM model, and the CNN-LSTM model, were constructed to predict the above six categories of risk-warning factors, and the predictive capabilities of the four models were compared and analyzed. The comparative results for the $RMSE$ and R^2 metrics are reported in Table 2 and Table 3, respectively.

The comparison shows that the CNN-ATT-LSTM model achieves better predictive performance than the CNN, LSTM, and CNN-LSTM models in terms of $RMSE$ and R^2 for the six risk-warning factors. Among these factors, because the first-bed temperature data of the synthesis tower itself exhibit relatively large oscillation amplitude and vibration frequency and are also affected by noise, the model does not learn the relevant features sufficiently well, resulting in an R^2 value of only 0.6042, which is lower than that of the other groups. However, the $RMSE$ result indicates that the deviation between the predicted value and the actual value remains relatively small. In addition, the comparison shown in Fig. 4 between the actual values and the predicted values suggests that the predicted results still satisfy practical requirements. The results show that the CNN-ATT-LSTM model is more capable of fully exploiting the hidden information among the data, accurately predicting the process parameters in the next 140 min, and providing a reliable data source for the early warning work.

Table 2: RMSE evaluation results of the prediction model

Risk warning factor	Predictive model *RMSE*			
	CNN	LSTM	CNN-LSTM	CNN-ATT-LSTM
Hydrogen-nitrogen ratio	0.0029	0.0019	0.0017	0.0009
Pressure at the inlet of the synthesis tower	4.6825	4.0142	2.2136	2.0174
The temperature of the first bed in the synthesis tower	0.2531	0.1413	0.1375	0.0739
Humidity of the second bed in the synthesis tower	0.1163	0.1002	0.0914	0.0896
Flow rate of condensate in the feed water heat exchanger	1.3748	1.0547	0.9631	0.8435
Pipeline process gas flow rate	5.4675	3.4124	2.5743	2.0142

Table 3: R^2 evaluation results of the prediction model

Risk warning factor	Predictive model R^2			
	CNN	LSTM	CNN-LSTM	CNN-ATT-LSTM
Hydrogen-nitrogen ratio	0.9755	0.9884	0.9941	0.9948
Pressure at the inlet of the synthesis tower	0.9425	0.9542	0.9793	0.9905
The temperature of the first bed in the synthesis tower	0.5673	0.5781	0.5936	0.6042
Humidity of the second bed in the synthesis tower	0.8694	0.8857	0.9234	0.9263
Flow rate of condensate in the feed water heat exchanger	0.7246	0.7591	0.8142	0.8345
Pipeline process gas flow rate	0.9941	0.9970	0.9974	0.9983

3.1.3 Analysis of risk prediction results

This paper refers to the enterprise DCS system alarm thresholds, while inviting one safety engineer and two process engineers to discuss the physical and chemical properties of the hazardous chemicals in the ammonia synthesis plant and the working data of the synthesis tower process device safety valves and pressure piping to get the risk thresholds of the six risk warning factors of the synthesis tower process part as shown in Table 4.

Table 4: Warning factor risk threshold

Parameters	L	I		II	
		I_1	I_h	II_1	II_h
Hydrogen-nitrogen ratio	(2.4,2.7)	(2.2,2.6]	(2.6,3)	[0,2.4)	(2.7,+∞)
Pressure at the inlet of the synthesis tower /kPa	(11300,13740)	(10200,12500]	(12500,14400)	[0,11300)	(13740,+∞)
The temperature of the first bed in the synthesis tower /℃	(495,504)	(491,500]	(500,509)	[0,495)	(504,+∞)
Humidity of the second bed in the synthesis tower /℃	(357,482)	(347,420]	(420,502)	[0,357)	(485,+∞)
Flow rate of condensate in the feed water heat exchanger /($t \cdot h^{-1}$)	(188,285)	(180,237]	(237,290)	[0,188)	(285,+∞)
Pipeline process gas flow rate /($km^3 \cdot h^{-1}$)	(505,695)	(485,600]	(600,710)	[0,505)	(695,+∞)

Based on the CNN-ATT-LSTM prediction results of risky warning factors, the risk level of each warning factor in the next 140 min is determined based on the risk thresholds in Table 4, and the risk associations of the 220 predicted data from the test set are plotted on a line to obtain the time-series risk affiliation of the warning factors in the next 140 min as shown in Fig. 5.

It is observed that the hydrogen-nitrogen ratio is at low risk for the next 140 min. The inlet pressure of the synthesis tower is high, which is in a class I risk state. The temperature of the first bed of the synthesis tower is high, and it is in the risk state of class I. The temperature of the second bed of the synthesis tower is low. The temperature of the second bed of the synthesis tower is low, and it is in the risk state of class I. It is necessary to pay attention so that the parameter values can be well controlled. Meanwhile, there are two risk changes in the condensate flow rate of feedwater heat exchanger in the next 140min. The condensate flow rate is larger in the first 130min and is in a Class I risk state, the Class I risk affiliation is 1 in the 26thmin, reaching the yellow alarm limit and issuing a yellow warning, and the condensate flow rate is too large and reaches a Class II risk state in the 130thmin. When the system issues a yellow warning, the enterprise operator should immediately take emergency measures to debug the condensate flow within the first 130min to prevent the risk level from rising continuously. If the control measures are not taken properly or emergency measures are not taken in time, resulting in the control parameter value reaching the Class II risk and the Class II risk affiliation degree is 1, the system issues a red warning signal, and the automation system will activate the emergency stopping measures by itself to prevent catastrophic accidents from occurring. In addition, there are two risk changes in the pipeline process gas flow in the next 140min. It rises from low risk to Class I risk, and the process gas flow rate is larger in the next 60min or so, which is in Class I risk status, and needs to be paid attention to, so that the parameter values can be well controlled.

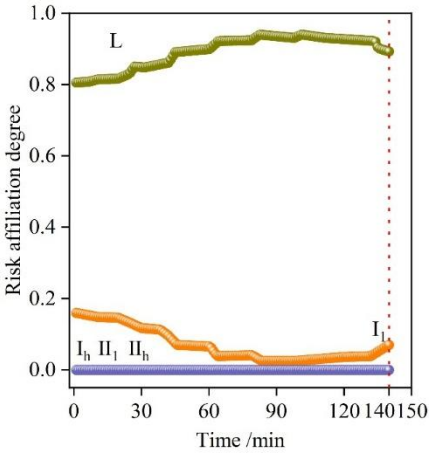

(a) Hydrogen-nitrogen ratio

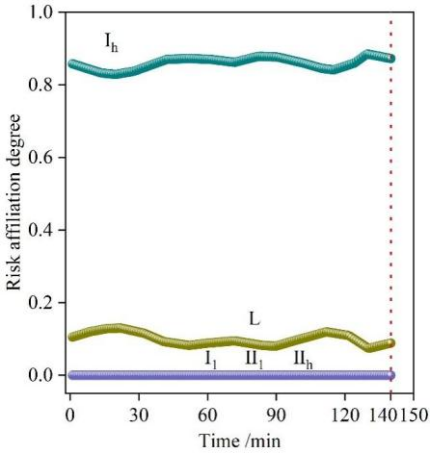

(b) Pressure at the inlet of the synthesis tower

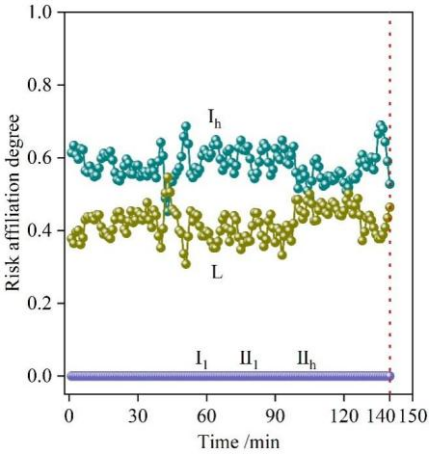

(c) The temperature of the first bed in the synthesis tower

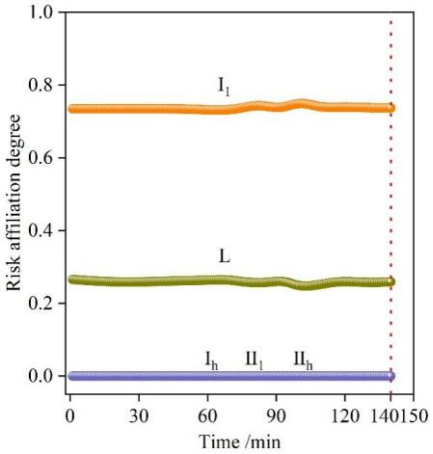

(d) The temperature of the second bed in the synthesis tower

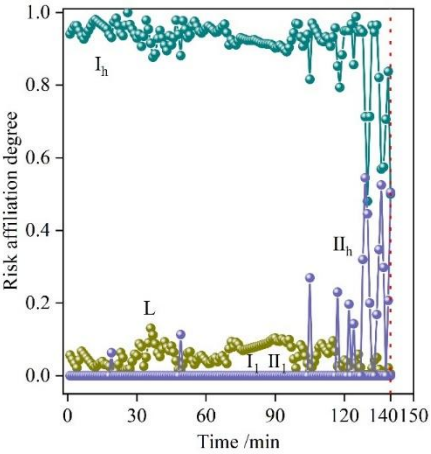

(e) Flow rate of condensate in the feed water heat exchanger

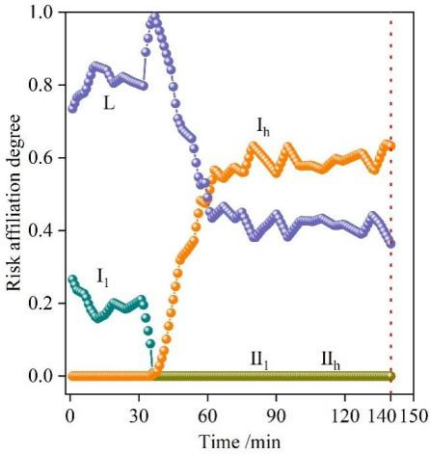

(f) Pipeline process gas flow rate

Figure 5: The change in the temporal risk membership degree of the early warning factor

3.2 BN safety risk traceability model construction and analysis

In this section, a Bayesian network model is constructed based on safety risk prediction prior to the chemical process, and safety risks are traced back after the fact.

3.2.1 Model construction and calculations

The process safety in the chemical production stage is selected as the target node to construct the Bayesian network, and the network structure is shown in Figure 6. Among them, each node has two states, “Yes” means that the node has appeared errors that may cause safety problems, and “No” means that the risk factors covered by the node are in normal operation.

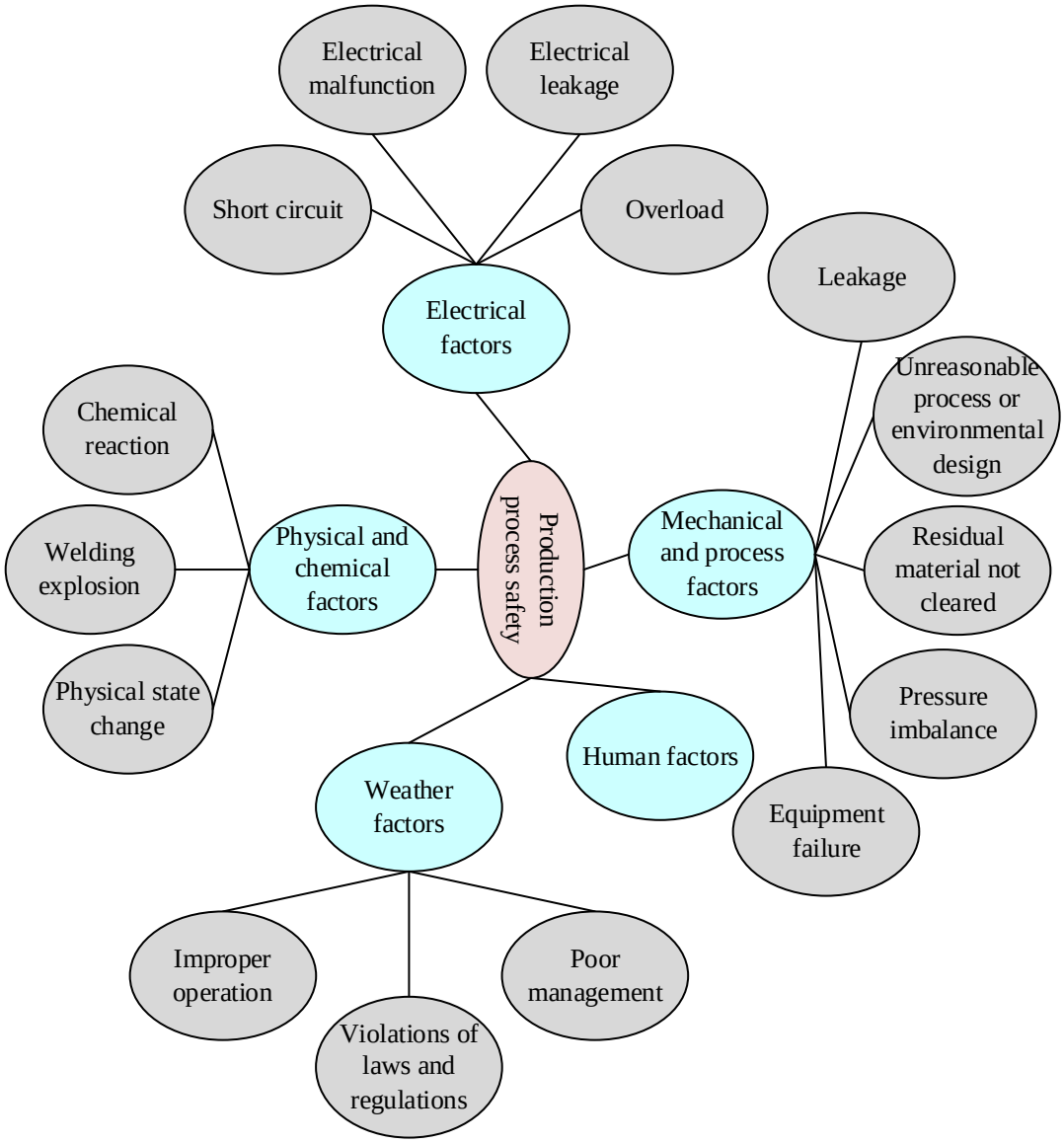

Figure 6: Bayesian network model for safety in chemical production processes

Based on the statistical information of each risk factor in the chemical-production stage, the prior probability of the parent node is derived from the occurrence frequency of secondary risk factors in that stage. In other words, the relationship between the occurrence frequency of risk factors and the prior probability $P(A)$ of a given node A can be obtained from Equation (25):

$$P(A) = n / N \tag{25}$$

where: n is the number of cases counted for the node A event, and N is the total number of cases counted for the production process, i.e. 220 cases.

According to the Bayesian conditional probability formula, the joint probability distribution formula for each node is obtained:

$$P\left(Y_1, Y_2, \cdots, Y_n\right) = \prod_{i=1}^{n} P\left(Y_i \mid T_i\right) \tag{26}$$

where: Y_i is each node in the network, n is the number of nodes, and T_i is the set of parents of Y_i.

Using GeNIe software, it updates the calculated prior probabilities of the parent node as well as the logical relationships between the nodes and uses the fixed-weight method to obtain the conditional probability distribution of each child node in order to determine the probability of the child node.

According to the calculation, according to the statistical data constructed in this model, the probability that safety problems may eventually occur in the chemical production stage is 15.04%, that is to say, when there is a risk hazard in a certain part of the chemical production process, there is a 15.04% possibility that it will lead to an accident. Constructing Bayesian network models for the other three stages separately according to the same model, the probabilities of problems in the storage, supply and transportation, installation and maintenance stages are obtained to be 10.86%, 18.93% and 20.74% respectively. It can be seen that the ability to resist risks in the storage stage is strong, while the ability to cope with risks in the installation and maintenance stage is weak, so attention should be paid to safety precautions in the installation and maintenance process to prevent risk factors from appearing as much as possible.

3.2.2 Model analysis and comparison

Still taking the production phase of the chemical process as an example, the degree of influence of the five main risk factors such as electrical, physicochemical, human, mechanical and process, and meteorological on the safety of the ammonia production process for the target event is considered. Reducing the probability of human error to 0%, i.e., discussing the safety of the production process in the absence of human risk factors in the production process, yields a probability of 2.51% that the production process will have a safety problem. Similarly changing the probability of error of physical and chemical, electrical, mechanical and process and meteorological factors respectively to 0%, the probability of safety problems in the production process is obtained to be 14.68%, 14.54%, 12.67%, 14.79%, i.e., the reduction of the human risk factors in the production phase can greatly reduce the emergence of safety problems, whereas the physical and chemical, electrical and meteorological factors have a safety accidents have less impact.

The probability of production process safety going wrong was changed to 100% for diagnostic reasoning analysis, i.e., the results of calculating the degree of influence that each primary and secondary factor may have on a production process safety accident when it occurs are shown in Table 5. It can be seen that human risk factors (85.74%) have the greatest impact on production process safety, followed by mechanical and process factors (22.35%).

Table 5: The degree of influence of risk factors on safety issues during the production stage

Main risk factors	Degree of influence	Measured value	Degree of influence
Human	85.74%	Poor management	8.25%
		Illegal and rule-breaking behaviors	58.97%
		Improper operation	49.38%
Electrical	4.62%	Short circuit	3.77%
		Electrical fault	3.41%
		Leakage current	3.78%
		Excessive load	0.76%
Meteorology	1.41%		
Physics and chemistry	2.86%	Chemical reaction	3.04%
		Explosion	1.63%
		Physical state changes	2.10%
Machinery and Technology	22.35%	Leakage	11.43%
		The process or environmental design is unreasonable	17.46%
		The remaining materials have not been cleared away	1.22%
		Pressure imbalance	3.31%
		Equipment failure	10.94%

Based on the information given, it is possible to state that the most significant reason behind the accidents in the chemical-production step is human factors. Human-related subfactors include illegal operation and improper operation which are the most influential ones. As per the outcome of the statistical analysis, 68 cases of accidents due to human factors make up 30.91 percent of the total number of accident samples, whereas illegal operation and improper operation represent 48.84 and 42.75 percent of the human factor accidents during the production phase, respectively. The proportions are relatively similar to the outcomes of the model analysis. Consequently, it is necessary to pay more attention to enhancing the safety measures of employees and instilling the spirit of safety in order to minimize the probability of accidents.

3.3 Early warning and decision-making on chemical process safety risks

Based on the results of chemical process safety risk prediction, this section proposes the following early warning scheme: through the construction of chemical process safety early warning knowledge map, the formation of a complete knowledge base containing monitoring sites, alarm thresholds, alarm processing solutions and other empirical knowledge and data, in order to provide knowledge support for the realization of early warning decision-making. By querying the safety warning thresholds, we can judge and analyze whether abnormal alarms will occur in the future state of the process parameters, and when abnormal alarms occur, we can provide processing solutions for the chemical site, so as to realize the function of early warning decision-making.

Taking a sensor node W9 in the ammonia synthesis section as an example, the relevant mapping information of monitoring locus W9 is shown in Fig. 7, which contains the associated four threshold entities, the interlock number entity, and the entity attributes. The bit represents the process parameter of the reflux tank level in the production line of the ammonia synthesis section, and its low threshold is 42, while the other thresholds do not exist, so they are all set to NA. There exists one kind of interlock number of the process parameter, which corresponds to the interlocking rule in the case of the low threshold, so that when the process parameter is lower than the set low threshold, the low-threshold alarm will be displayed, and then

corresponding interlocking reaction will be made, thus preventing the occurrence of production accidents.

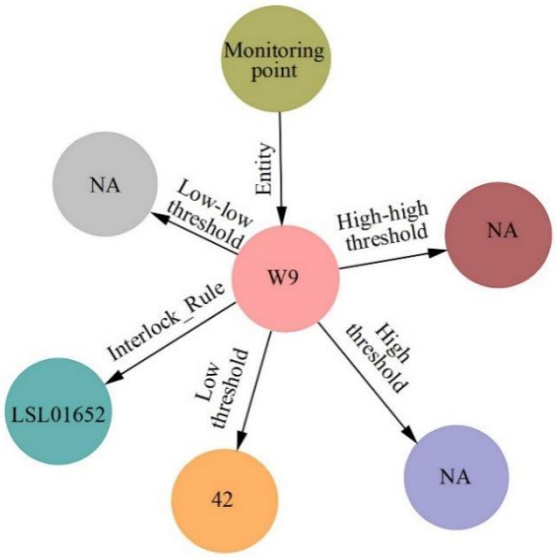

Figure 7: Knowledge graph of sensor W9

At the same time, the results predicted by the CNN-ATT-LSTM-BN model can be provided with a certain degree of interpretability and dynamically updated into the knowledge graph to realize the visualization of the dynamic correlation between the process parameters under different temporal states, which provides the basis for correlation analysis for the real-time monitoring and control process of the chemical production site. The correlation between the process parameters of the reflux tank level in ammonia synthesis process and other process parameters at different production stages is shown in Fig. 8, which is derived from the results obtained from the convolution kernel learning in the CNN-ATT-LSTM-BN model. From the figure, it can be seen that the correlation weights of different process parameters associated with the reflux tank level under different time periods are dynamically changed.

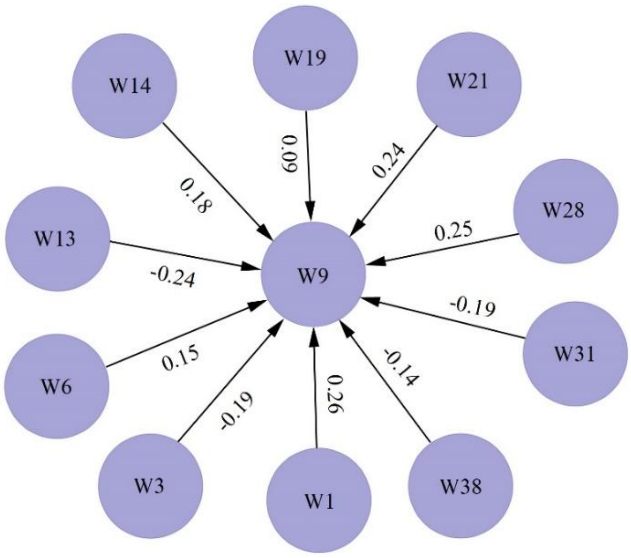

Figure 8: Correlation between the liquid level of the reflux tank and other parameters

4 Conclusion

Based on the safety-risk early-warning problem of chemical processes, this paper suggests a risk-warning model called as CNN-ATT-LSTM-BN, consisting of both a CNN-ATT-LSTM predictor model and a BN-based risk-tracer model. It is also validated that the model is valid and a decision-making plan to warn about risks is also suggested.

The CNN-ATT-LSTM model achieves its best predictive accuracy during 550 training rounds and a maximum of 5500 iterations whereby the R^2 and $RMSE$ values are 0.98794 and 0.00088 respectively. In case the model was used to predict six chemical-process parameters the resulting R^2 and $RMSE$ values were better than those achieved by the CNN, LSTM, and CNN-LSTM models and the prediction accuracy was high enough to be applied in practice. The forecast shows that the hydrogen-nitrogen ratio will be at a low-risk level over the next 140 minutes. The synthesis tower inlet pressure, as well as the first and second bed temperatures, are categorized as Class I risk and thus must be controlled properly. The condensate flow rate is also in a Class I risk condition initially (the first 130 minutes) and then changes to Class II risk conditions (emergency action should be taken immediately to stop the risk level increasing).

According to the BN model, the probability that safety problems may eventually occur in the production, storage, supply and transportation, and installation and maintenance phases of a chemical process is 15.04%, 10.86%, 18.93%, and 20.74%, respectively. Among them, the storage stage is more resistant to risks, while the installation and maintenance stage is less capable of coping with risks, so the safety precautions in the installation and maintenance process should be emphasized to prevent risk factors from appearing as much as possible. In addition, in the production stage, the greatest influence on chemical process safety is human risk factors (85.74%), followed by mechanical and process factors (22.35%).

Based on the results of chemical process safety risk prediction, this paper proposes a safety risk early warning decision-making program. That is, through the construction of chemical process safety early warning knowledge map, the formation of a complete knowledge base containing monitoring points, alarm thresholds, alarm processing programs and other empirical knowledge and data, to provide knowledge support for the realization of early warning decision-making.

About the Author

Shuai Meng was born in Fushun, Liaoning, P.R. China, in 1982. He obtained a master's degree from Liaoning Petrochemical University in China. I am working at the School of Department of chemical engineering, Fushun Vocational Technology Institute. My main research direction is Chemical engineering and Chemical Instrumentation.

References

[1] Han, H., Yang, Y., Zhang, R., & Brekhna, B. (2020). Factors and paths of transformation and upgradation of chemical industry in Shandong, China. Sustainability, 12(8), 3443.

[2] Hong, S., Jie, Y., Li, X., & Liu, N. (2019). China’s chemical industry: new strategies for a new era. McKinsey & Company.

[3] Agarwal, P., Goyal, A., & Vaishnav, R. (2018). Chemical hazards in pharmaceutical

industry: An overview. Asian J. Pharm. Clin. Res, 11(2).

[4] Lebelo, K., Malebo, N., Mochane, M. J., & Masinde, M. (2021). Chemical contamination pathways and the food safety implications along the various stages of food production: a review. International journal of environmental research and public health, 18(11), 5795.

[5] Chen, C., & Reniers, G. (2020). Chemical industry in China: The current status, safety problems, and pathways for future sustainable development. Safety science, 128, 104741.

[6] Dakkoune, A., Vernières-Hassimi, L., Leveneur, S., Lefebvre, D., & Estel, L. (2018). Risk analysis of French chemical industry. Safety science, 105, 77-85.

[7] Duan, W., Chen, G., Ye, Q., & Chen, Q. (2011). The situation of hazardous chemical accidents in China between 2000 and 2006. Journal of hazardous materials, 186(2-3), 1489-1494.

[8] Wang, B., Wu, C., Reniers, G., Huang, L., Kang, L., & Zhang, L. (2018). The future of hazardous chemical safety in China: Opportunities, problems, challenges and tasks. Science of the total environment, 643, 1-11.

[9] Jung, S., Woo, J., & Kang, C. (2020). Analysis of severe industrial accidents caused by hazardous chemicals in South Korea from January 2008 to June 2018. Safety science, 124, 104580.

[10] Duka, G. (2017). Ecological & Environmental Chemistry. In Ecological and environmental chemistry (pp. 11-20).

[11] Li, Z., Yao, M., Luo, Z., Wang, X., Huang, Q., & Su, C. (2023). Analysis of risk factors of coal chemical enterprises based on text mining. Journal of environmental and public health, 2023(1), 4181159.

[12] Lampadarios, E. (2016). Critical challenges for SMEs in the UK chemical distribution industry. Journal of Business Chemistry, 13(1).

[13] Bhusnure, O. G., Dongare, R. B., Gholve, S. B., & Giram, P. S. (2018). Chemical hazards and safety management in pharmaceutical industry. Journal of Pharmacy Research, 12(3), 357-369.

[14] Ayeni, O., & Olagoke-Komolafe, O. E. (2024). Advancing chemical safety protocols in small and medium enterprises: A comprehensive guide. CRR Journals, 2(1), 47-60.

[15] Sonawane, S. L., Patil, V. J., & Tigaa, R. A. (2022). Evaluating and promoting chemical safety awareness in the chemical sciences. Journal of Chemical Education, 100(2), 469-478.

[16] Ostad-Ali-Askari, K. (2022). Management of risks substances and sustainable development. Applied Water Science, 12(4), 65.

[17] Bai, M., Qi, M., Shu, C. M., Reniers, G., Khan, F., Chen, C., & Liu, Y. (2023). Why do major chemical accidents still happen in China: Analysis from a process safety management perspective. Process safety and environmental protection, 176, 411-420.

[18] Wang, Y., Henriksen, T., Deo, M., & Mentzer, R. A. (2021). Factors contributing to US chemical plant process safety incidents from 2010 to 2020. Journal of Loss Prevention in the Process Industries, 71, 104512.

[19] Kidam, K., & Hurme, M. (2013). Analysis of equipment failures as contributors to chemical process accidents. Process Safety and Environmental Protection, 91(1-2), 61-78.

[20] Butnariu, M., & Bonciu, E. (2022). Assessment of some hazards associated with dangerous chemicals. In Environmental biotechnology (pp. 1-37). Apple Academic Press.

[21] Peres, R. S., Jia, X., Lee, J., Sun, K., Colombo, A. W., & Barata, J. (2020). Industrial artificial intelligence in industry 4.0-systematic review, challenges and outlook. IEEE access, 8, 220121-220139.

[22] Lee, J., Davari, H., Singh, J., & Pandhare, V. (2018). Industrial Artificial Intelligence for industry 4.0-based manufacturing systems. Manufacturing letters, 18, 20-23.

[23] Kraus, N., Kraus, K., Shtepa, O., Hryhorkiv, M., & Kuzmuk, I. (2022). Artificial intelligence in established of industry 4.0. WSEAS transactions on business and economics, (19), 1884-1900.

[24] Javaid, M., Haleem, A., Singh, R. P., & Suman, R. (2022). Artificial intelligence applications for industry 4.0: A literature-based study. Journal of Industrial Integration and Management, 7(01), 83-111.

[25] Konrad, A. (2024). How artificial intelligence can be used in the chemical industry. Journal of Business Chemistry, 21(2).

[26] Chiang, L. H., Braun, B., Wang, Z., & Castillo, I. (2022). Towards artificial intelligence at scale in the chemical industry. AIChE Journal, 68(6), e17644.

[27] Oliveira, L. M., Dias, R., Rebello, C. M., Martins, M. A., Rodrigues, A. E., Ribeiro, A. M., & Nogueira, I. B. (2021). Artificial intelligence and cyber-physical systems: A review and perspectives for the future in the chemical industry. AI, 2(3), 27

[28] Liao, M., Lan, K., & Yao, Y. (2022). Sustainability implications of artificial intelligence in the chemical industry: A conceptual framework. Journal of industrial ecology, 26(1), 164-182.

[29] Wang, Y. (2022). Safety production supervision of industrial enterprises based on deep learning and artificial intelligence. Mobile Information Systems, 2022(1), 1820082.

[30] Roy, A., Srivastava, P., & Sinha, S. (2014). Risk and reliability assessment in chemical process industries using Bayesian methods. Reviews in Chemical Engineering, 30(5), 479-499.

[31] Yazdi, M., & Kabir, S. (2017). A fuzzy Bayesian network approach for risk analysis in process industries. Process safety and environmental protection, 111, 507-519.

[32] Chen, S. H., & Pollino, C. A. (2012). Good practice in Bayesian network modelling.

Environmental Modelling & Software, 37, 134-145.

[33] Mohammadfam, I., Ghasemi, F., Kalatpour, O., & Moghimbeigi, A. (2017). Constructing a Bayesian network model for improving safety behavior of employees at workplaces. Applied ergonomics, 58, 35-47.

[34] Marcot, B. G., & Penman, T. D. (2019). Advances in Bayesian network modelling: Integration of modelling technologies. Environmental modelling & software, 111, 386-393.

[35] Kitson, N. K., Constantinou, A. C., Guo, Z., Liu, Y., & Chobtham, K. (2023). A survey of Bayesian Network structure learning. Artificial Intelligence Review, 56(8), 8721-8814.

[36] Zarei, E., Khakzad, N., Cozzani, V., & Reniers, G. (2019). Safety analysis of process systems using Fuzzy Bayesian Network (FBN). Journal of loss prevention in the process industries, 57, 7-16.

[37] Sýkora, M., Markova, J., & Diamantidis, D. (2018). Bayesian network application for the risk assessment of existing energy production units. Reliability Engineering & System Safety, 169, 312-320.

[38] Yu, R., & Zhang, C. (2021). Early warning of water quality degradation: A copula-based Bayesian network model for highly efficient water quality risk assessment. Journal of environmental management, 292, 112749.

[39] Barua, S., Gao, X., Pasman, H., & Mannan, M. S. (2016). Bayesian network based dynamic operational risk assessment. Journal of Loss Prevention in the Process Industries, 41, 399-410.

[40] Wang, X., Xue, X., Yeoh, W., Sun, X., & Qin, H. (2025). Risk propagation analysis of domino effect in chemical accident: An integrated approach with data mining and Bayesian networks. Journal of Loss Prevention in the Process Industries, 105745.

[41] Zerrouki, H., & Smadi, H. (2017). Bayesian belief network used in the chemical and process industry: a review and application. Journal of Failure Analysis and Prevention, 17(1), 159-165.

[42] Lu, Y., Wang, T., & Liu, T. (2020). Bayesian network-based risk analysis of chemical plant explosion accidents. International journal of environmental research and public health, 17(15), 5364.

[43] Zhu, R., Li, X., Hu, X., & Hu, D. (2019). Risk analysis of chemical plant explosion accidents based on Bayesian network. Sustainability, 12(1), 137.

[44] Zhou, Z., Huang, J., Lu, Y., Ma, H., Li, W., & Chen, J. (2022). A new text-mining–Bayesian network approach for identifying chemical safety risk factors. Mathematics, 10(24), 4815.

[45] Zarei, E., Mohammadfam, I., Azadeh, A., Khakzad, N., & Mirzai, M. (2018). Dynamic risk assessment of chemical process systems using Bayesian Network. Iran Occupational Health, 15(3), 103-117.

[46] Ying, Y. (2023, October). Research on Risk Calculation in Chemical Production Processes Based on Dynamic Bayesian Networks. In 2023 IEEE 14th International Conference on Software Engineering and Service Science (ICSESS) (pp. 33-37). IEEE.

[47] Zhou, Z., Guo, J., & Huang, J. (2025). Chemical Safety Risk Identification and Analysis Based on Improved LDA Topic Model and Bayesian Networks. Applied Sciences, 15(11), 6197.

[48] Lv, C., Wang, X., Xue, S., & Wang, S. (2025). Investigation of risk-aware dynamic accident monitoring and early warning technologies for chemical production processes. Scientific Reports, 15(1), 9466.